MODULAR AFFORDABLE GPS/INS (MAGI)

Dr. Mahendra Singh
WADDAN SYSTEMS

Stuart McNamee
412TW/TSD

Allen Khosrowabadi
Tybrin Corporation

ABSTRACT

The GPS/INS equipment is used at the Air Force Flight Test Center (AFFTC) to collect time space position information (TSPI) during testing. The GPS-based test instrumentation is lagging behind available commercial technologies. Advancing technologies for test use requires investigation of affordable commercial equipment. To enable technology insertion for state of the art testing, there is a need for more robust, flexible, reliable, modular, affordable low cost TSPI systems capable of operating in all flight environments. Modular (plug-and-play) hardware and software, quick and easy to re-configure, are required for supporting various test platforms from fighter aircraft to cargo size aircraft. Flight testing dynamics are such that, GPS-only systems tend to lose data during critical maneuvers. To minimize this data loss, inertial measurement systems coupled with GPS sensors are used in most sophisticated range instrumentation packages. However, these packages have required fairly expensive inertial units, are usually very large and not very flexible in terms of quick and easy reconfiguration to meet the unique needs of AFFTC's test customers. WADDAN SYSTEMS has begun to address this problem with a modular design concept, which incorporates their high-performance navigation quality inertial measurement unit, but with costs comparative to that of lower-end performance inertial units. This paper describes WADDAN's concept and the components that make up MAGI; and addresses some of the preliminary testing and near-term proposed activities. In general, the system will provide GPS, inertial and discrete MIL-STD 1553, RS-232/422 and video data from the participant. The MAGI will be structured around the Compact personal computer interface (PCI) backplane bus with on-board recording and processing and will include real-time command and control through a UHF data link.

KEY WORDS

GPS/INS, CompactPCI, MEMS, Inertial Sensors, IMU, Gyro, Accelerometer, Silicon Sensors

INTRODUCTION

Currently the Air Force Flight Test Center (AFFTC) employs time space position and information (TSPI) range instruments that are housed in PODs (i.e., AIM 9 housings) or strapped to plates (i.e., box enclosures). A typical system consists of discrete assemblies of AC/DC power supply, GPS receiver and antenna, inertial reference or inertial measurement unit's (IRU/IMU), data link transceiver, range encryption module (REM), intelligent flash solid-state recorder (IFSSR), advanced digital interface unit (ADIU), isolation box, etc. These TSPI systems that support dynamic testing have found tightly coupled GPS and inertial systems work best. The performance and cost driver of these systems is the inertial unit's. Generally, there are standard configurations with frozen designs. Updates and reconfigurations are difficult, as insertion of improved and advancing technologies can not be done without a major redesign effort. Although the computer system technology in the commercial arena is advancing very rapidly, the same is not true with the technology employed in the TSPI systems. Hence, there is a need for a robust, flexible, reliable, modular, low cost TSPI system capable of operating in a low-to-high dynamic flight environment. The system should have plug-and-play modular hardware and software, in order to quickly reconfigure among different airframes. It should be able to mount in internal equipment bays of fighter, trainer, and cargo size military aircraft.

WADDAN SYSTEMS has begun the development of a modular affordable GPS/INS (MAGI) as shown in Figure 1. After comparing various commercial-off-the-shelf (COTS) component technologies, a compact PCI-based system was conceived. It utilizes a backplane, which interfaces with all the system modules. The heart of the system operation and control is the CPU board, but performance and cost drive the inertial unit. Currently a board populated by a Pentium class processor with 128 MB RAM, 512 KB cache, video, keyboard, mouse, serial and parallel ports, interface connectors for Ethernet, universal serial board (USB) and FireWire. Other modules that can be plugged into the backplane include a GPS board, a solid-state memory board, a data acquisition board, data link board and an inertial measurement unit (IMU) board. As per compact PCI specifications, all these modules and the system CPU module are plug-and-play compatible.

Again, the performance and cost driver of MAGI is its IMU. The IMU performance and cost are directly proportional to fabrication and manufacturing processes and techniques. An inertial sensor, AXLGYRO, is a low cost IMU module for MAGI. It is a silicon device consisting of a pendulous accelerometer and a tuned fluttering gyro built together

on a single chip. Three fabrication iterations have been completed to iron out manufacturing process problems. These devices have been tested for functionality. A Kalman filtering technique was developed for real-time integration of the GPS/INS data.

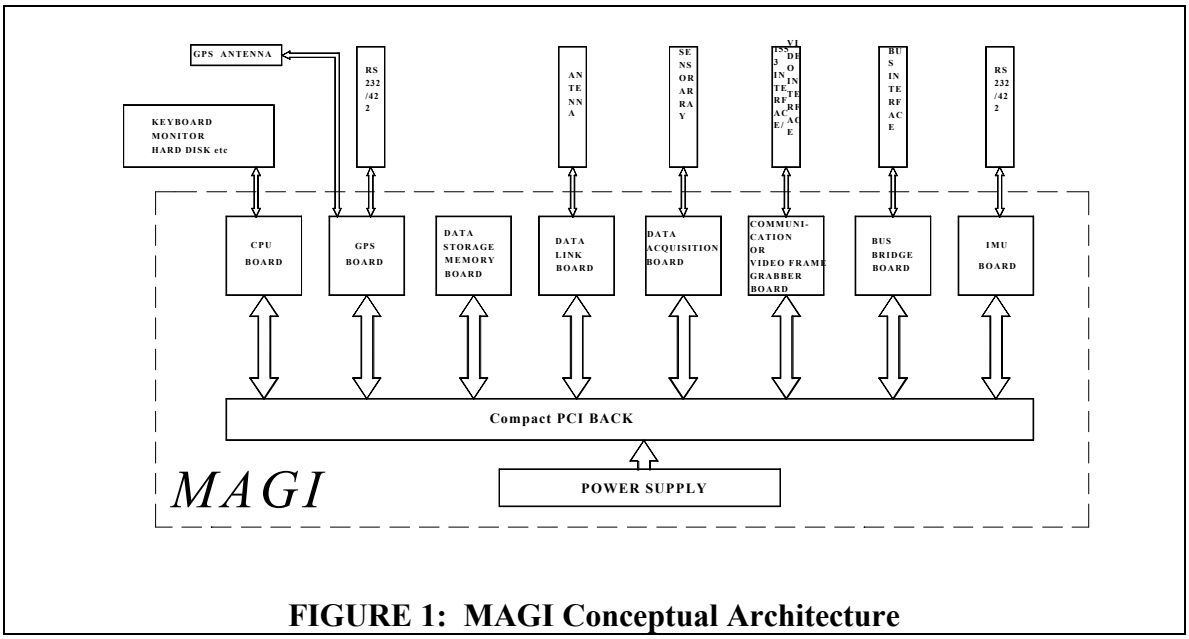

FIGURE 1: MAGI Conceptual Architecture

The production goals for the system conceived are listed in Table I.

TABLE I: MAGI PRODUCTION GOALS

Size (mm x mm x mm)	125x125x200
Power (watts)	30
IMU Cost per unit (K$) (Gyro: 1 °/hr, Accel: 300 μG)	2
Cost per system (K$)	10

OVERVIEW OF MAGI

The system architecture for MAGI is based upon the compact PCI bus structure that provides a high speed bus with plug-and-play capability in hardware as well as software. The bus is designed for surviving the harsh industrial environment. All modular boards used in MAGI have a set of 256 registers containing information on the board identity, and programmable parameters such as address maps, or interrupt types and levels. The operating system auto-detects a board in the system and configures it without the need of jumpers or switches. This allows MAGI to be *auto-reconfigurable* with any set of

modular boards employed in the system for a desired test scenario. The plug-and-play capabilities of MAGI are summarized in Table II.

TABLE II: MAGI PLUG-AND-PLAY CAPABILITIES

TECHNOLOGY UPGRADE/REPLACEMENT	HARDWARE MOD	SOFTWARE MOD
Backplane	Chassis	None
CPU Board (Pentium/PowerPC/Alpha)	None	None
GPS Board	None	Board Driver and GPS/IMU Kalman Filter Application
Solid-State Memory Board	None	None
Data Acquisition Board	None	Board Driver and Data Acquisition Application
RF Data Link Board	None	Board Driver and Transceiver Application
IMU Module	None	Board Driver and GPS/IMU Kalman Filter Application
Operating System	None	Board Drivers
Dedicated MAGI Software Application	None	None

A configuration of MAGI is shown in Figure 2. The system consists of the eight modules shown vertically, each locked in place. The leftmost board is the system CPU board so it has to be present at all times like the motherboard in a PC. The other seven slots are populated with peripheral boards, which may or may not be plugged in. The system is flexible enough so that these modular boards could be plugged in any order; however, at this stage of development the first slot on the left side in the illustration is reserved for the CPU board, and the last slot to the right is dedicated to the IMU board. The latter is done to accommodate the different sizes of the IMU sensor blocks without interfering with any adjoining board.

The second board from the left is a GPS receiver. Depending upon the hardware and software designs associated with the GPS board, the time tagged raw data could be stored in the memory module via the CPU or directly with direct memory access (DMA). The data could also be transmitted to a ground station. Additionally, the raw data could be integrated with the IMU data to yield a real-time integrated TSPI solution. The third board on the backplane is flash memory to store the data collected and processed during the flight. The fourth module is a data link transceiver that could transmit or receive data to or from ground stations during the test flight. The fifth module is a data acquisition board to collect data from various analog/digital sensors such as temperature probes, strain gages, shock/vibration accelerometers, humidity sensors, ice detectors, radiation

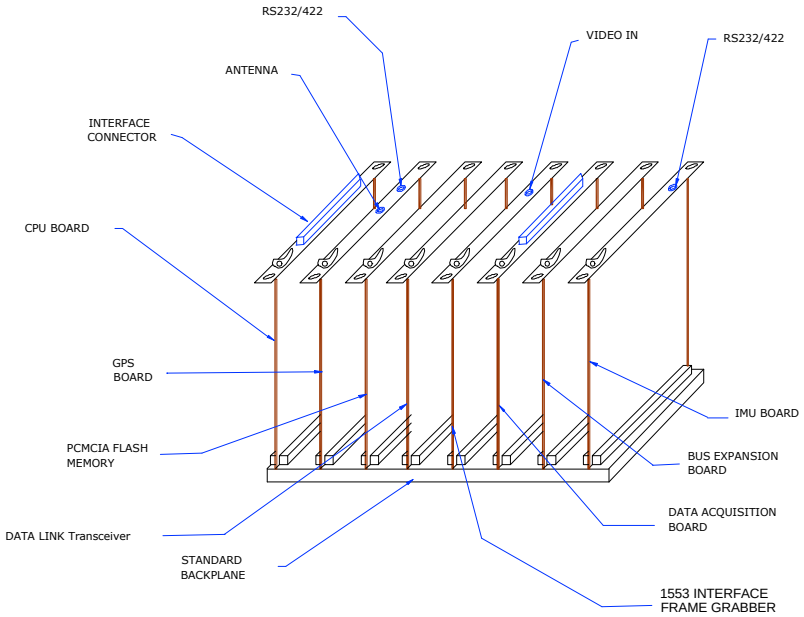

Figure 2: MAGI System Concept

sensors, etc. The sixth and seventh slots can accommodate either an interface board for 1553 bus or a video frame grabber attached to video cameras or bus bridge board. The latter is employed when the system needs to be expanded to include more boards housed in a different chassis. The last board at the end is an IMU board with a triad of gyros and accelerometers along with their support electronics for sampling these inertial sensors at a given rate.

IMU

Out of all the peripheral boards this is the only one which is not yet a COTS component. WADDAN SYSTEMS has begun the development of an IMU board meeting the compact PCI specifications. The board layout along with the sensor block is illustrated in Figure 3. An orthogonal triad of the AXLGYRO sensor forms the sensor block. The sensor is an integrated silicon device with a pendulous accelerometer and dithering gyro built together on the same chip. Although the initial planning calls for the sensor block to be assembled on the IMU board, it might be necessary to move it off the board to minimize vibration-induced problems. Therefore, as a contingency, the last slot of the backplane is reserved for the IMU board so that the sensor block can be mounted on a ruggedized chassis wall to minimize the shock and vibration related errors.

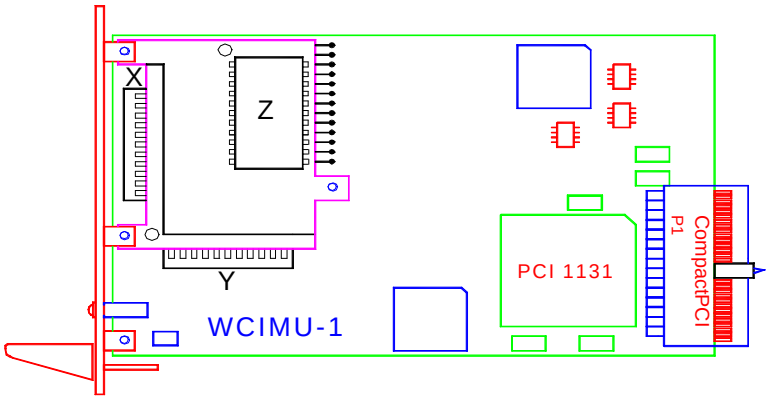

Figure 3: WADDAN SYSTEMS' Compact PCI IMU Board Layout

In essence, the AXLGYRO chip replaces a traditional accelerometer and a gyro having input axes parallel to each other. Both the accelerometer and the gyro are closed loop devices with a pickoff and an electrostatic forcer or torquer. The forcing action is controlled by a pulse width modulated (PWM) approach that produces a pseudo digital output.

When the device is strapped to a body, the outer frames of both the devices move along with the body, but the sensing element in each due to its inertia tends to stay where it is, thus, creating a relative *position differential* with respect to its frame. This *position differential* is determined by the change in the pickoff signal. The PWM servo electrostatically forces the sensing element to a position such that its relative *position differential* vanishes by attaining the pickoff signal level corresponding to the null position. The effort required to achieve this null positioning is proportional to the acceleration or the rate being sensed.

These AXLGYROs are fabricated using mature technologies that WADDAN SYSTEMS has developed over the last decade. At the present stage of development, the AXLGYRO servo electronics are off-chip ICs. A photo of this AXLGYRO is shown in Figure 4. The sensing element and its surrounding structure are all machined in <100> bulk silicon, which is sandwiched between Pyrex glass plates with forcing electrodes. The entire device measures approximately 12x20x1.8 mm^3. The sensitive axes of both the devices are normal to the wafer or the photo. The pickoffs in the device consist of differential parallel plate capacitors. All restoring torques are applied using differential

electrostatic forces. Because of the high aspect ratio structures and the hard stops utilized in the design, the sensors can be very accurate, and yet capable of surviving harsh environments.

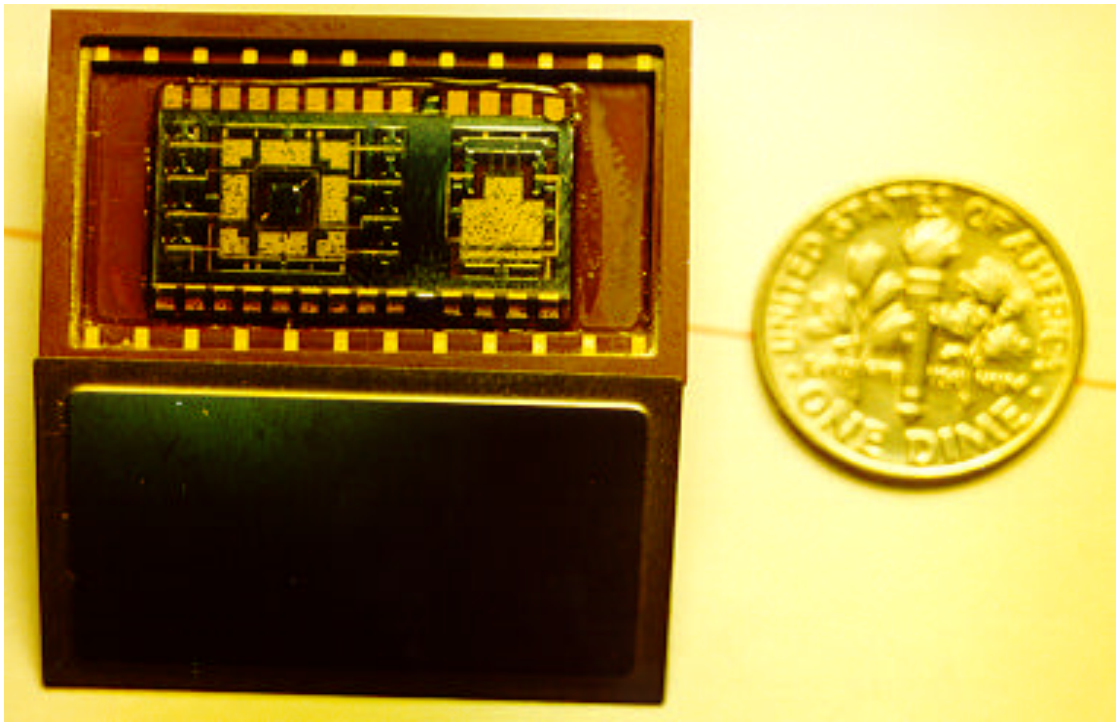

FIGURE 4: A Packaging Scheme for AXLGYRO

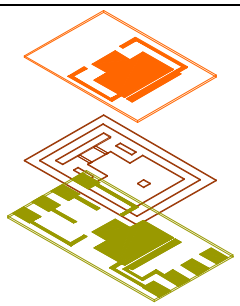

FIGURE 5: Three Plates Forming the Accelerometer

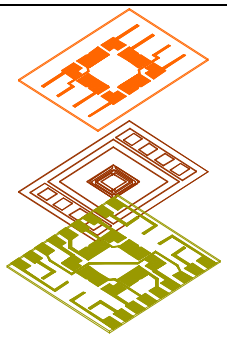

FIGURE 6: Three Plates Forming the Gyro

A three-dimensional model of the accelerometer is shown in Figure 5. It consists of two thin hinges that provide the pendulous proofmass with a rotational degree of freedom about an axis normal to their length. Most of the mass is concentrated away from the hinges in the rectangular plate structure. In turn, this entire structure is supported by an electrically isolated island. The silicon plate is sandwiched between two glass plates with metalized electrodes facing the silicon. The proof mass also has electrodes integrally fabricated in it that face the glass

$$m\ddot{Y} = -K_v v = -\frac{2eAV_0}{s^2} v$$

$$\ddot{Y} = -\left[\frac{2eAV_0}{ms^2}\right] v$$

electrodes. The two pairs of smaller electrodes farthest from the hinge serve as a differential pickoff, and two larger pairs provide the electrostatic forces for rebalancing the proofmass to its null position. If the servo applies the electrostatic force in such a way that the mass *m* is forced back to its null position, then the inertial force equals the electrostatic force as shown in the adjoining box.

A three-dimensional model of the gyro is shown in Figure 6. The sensing element is fabricated in bulk silicon and is sandwiched between two glass plates. The glass plates have gold plated electrodes for pickoff and forcing action. The sensing element of the gyro consists of a square flutter inertia supported by a mechanical structure consisting of two orthogonal gimbals made out of very thin silicon structures. The gimbal structure supported by an electrically isolated pedestal provides the flutter with 2 degrees of limited freedom about two in-plane axes perpendicular to each other.

This gyro could be considered an AC analog of the classical spinning wheel gyro. Instead of having a spin axis, it has a dither axis, about which the angular velocity of the flutter is *precisely* modulated. Thus, instead of a constant angular momentum, one deals with a modulated angular momentum of a *constant amplitude at a known frequency*. The input axis (IA) of the device is normal to the plane of the flutter. When the sensor is exposed to a DC angular rate along the input axis, it introduces a change in the angular momentum proportional to the applied rate about an axis normal to both the applied rate and the angular momentum vectors, i.e., the output axis. This change in the angular momentum vector is actually an angular acceleration about the output axis; that produces an inertial torque acting on the flutter. Since the angular momentum is modulating, this inertial torque is also modulating at the same frequency.

This causes torsional oscillations in the flutter about the output axis. In the close loop mechanization, an alternating rebalance torque is applied to the flutter through its forcer electrodes to drive it back to its *rotationally null position* (with vanishing rotations) about the output axis. The differential amplitude of the rebalance torque necessary to achieve this nulling is directly proportional to the angular rate input.

$$J_c \Omega_Z \omega_D \left[\frac{K_{dV} v_{d0}}{-J_x \omega_D^2 + 2k_x + K_{dq}}\right] = -K_{FV} v_{f0}$$

$$\Omega_Z = \frac{-K_{FV} v_{f0}}{J_c q_0 \omega_D} = -\left[\frac{4eA_f D_f}{J_c s^2}\right]\left(\frac{V_0}{q_0 \omega_D}\right) v_{f0}$$

If the applied rebalancing voltage, $v_f = v_{f0}\cos(\omega_D t)$, is such that the rotor is driven back to its null, then the relationship in shown in the adjoining box can be obtained by equating the gyroscopic torque with the rebalancing torque.

In the preceding equation, the term, $\left[\frac{K_{dV} v_{d0}}{-J_x \omega_D^2 + 2k_x + K_{dq}}\right]$, actually represents the uncoupled dither amplitude, q_0, which is a constant based upon the structural resonant

characteristics of the gimbal flexure. Thus, the *amplitude* of the balancing voltage, v_{f0}, is a direct measure of the angular rate, Ω_Z.

The functionality of the AXLGYRO was tested using one of the devices from Batch # 2. A fine wire was bonded to each one of the device pads using a conductive epoxy. Next, the device was cemented on a 24 pin DIP socket. The free ends of the wires connected to the device were soldered to the pin heads of the DIP socket. A photo of the device used in the tests is shown in Figure 7.

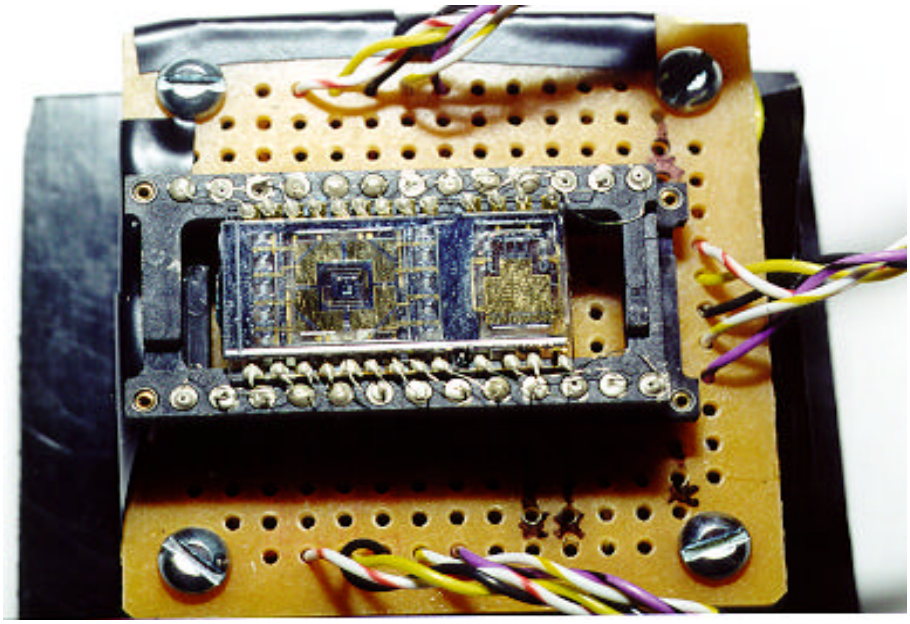

FIGURE 7: Photo of a Device Used in Functionality Tests

Three different cross-sections of the device with planes perpendicular to the wafer are shown in Figure 8. The cross-section BB shows the gyro flutter supported by a hub in the center about which the flutter can oscillate. Four pickoffs are located at the outside corner tips of the flutter, two on the top and two on the bottom side. Two forcers are located on the either side in between the pickoff and the gimbal structure. When the flutter oscillates, the pickoffs that are diagonally across experience similar effects, either increasing or decreasing capacitance. The pickoffs. top pickoffs (TPO) and bottom pickoffs (BPO), that are diagonally across are shorted together. When the capacitance of the one diagonal pair of pickoffs (represented by TPO) increases, then that of the other diagonal pair (represented by BPO) decreases. The differential value of the TPO and BPO signals yields the net pickoff signals used by the servo to generate appropriate voltages at the forcer electrodes for rebalancing. Again, since the forcer pair located diagonally across the flutter is required to develop similar forcing actions, the pair is shorted together.

The cross-section AA shows a view identical to that of cross-section BB with equal number of pickoffs and forcers. However, the forcers shown in this view are employed to

impart a constant sinusoidal angular momentum to the flutter. It should also be noted, that in this case, also the forcers providing similar actions are shorted together.

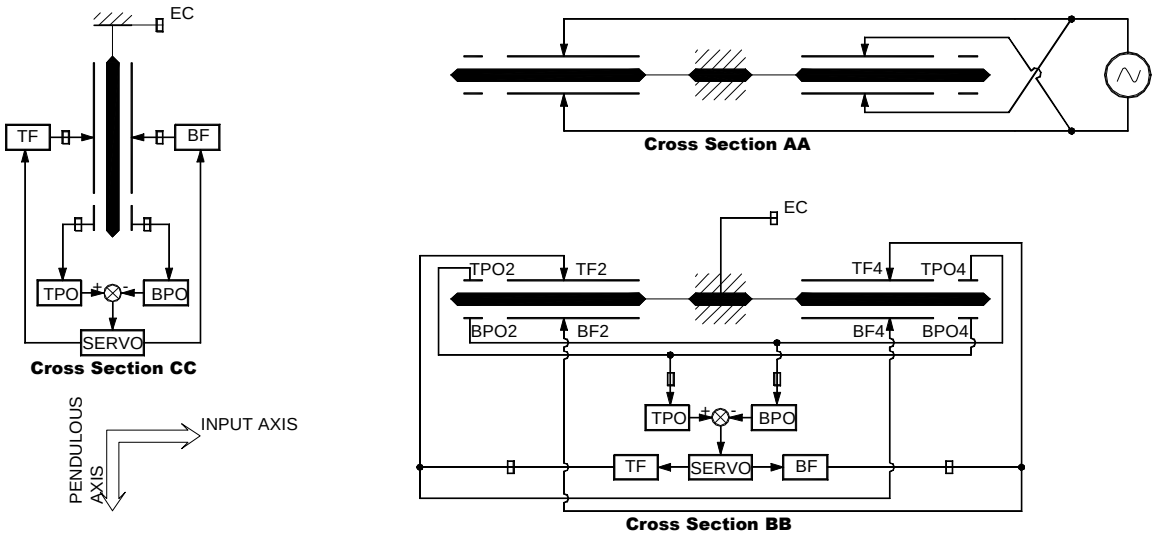

FIGURE 8: AXLGYRO Sensing Element Cross-Sections with Servo Loops

The forcers shown in cross-section AA were connected to a function generator set at 100 Hz for sine wave output. This excitation imparted the sinusoidal motion to the flutter about an axis lying in the plane of the wafer and perpendicular to cross-section AA. This axis is referred to as the dither axis of the gyro. The rebalancing servo electronics was hooked up as shown in cross-section BB. (The rebalancing action takes place about the output axis). The net differential pickoff signal and the voltage required for forcing were monitored by an oscilloscope. The pickoff signal was found to be a low amplitude sinusoidal signal lagging approximately 90 degrees with respect to dither drive signal. It compared well with the theory, which predicted a 90-degree phase lag with no mechanical damping in the device. The device actually has some desirable damping due to the dry nitrogen trapped inside during the glass bonding operation. Next the device was subjected to an angular rate pulse about the input axis. The forcer signal was observed to follow the rise and fall of the pulse input.

The cross-section CC in the figure shows a view through the accelerometer proofmass. In this case, there are two pickoffs located at the free end of the proofmass. When the proofmass moves out of its null position, the capacitance on the side with smaller gap (e.g., TPO) increases, and that on the other side (BPO) decreases. A differential signal between TPO and BPO yields the net pickoff signal used by the servo to generate the required forcing action. Nominally, under zero acceleration input, the servo generates equal but opposite forces TF and BF on the forcers, but as soon as a non-zero pickoff signal is provided, the servo makes the differential force between top force (TF) and bottom force (BF) such that the pickoff signal becomes vanishingly small. The accelerometer was connected to the servo electronics as shown in FIGURE 8. In open loop, when the forcing voltage was changed from 1 extreme to another, the pickoff signal

was found to follow the change. After nulling the device in the zero g position, the device was turned approximately to positive 1 g position, and the value of the forcer output was observed. Then the device was turned approximately to -1 g position, and again the value of the forcer voltage was observed. The average change between the extreme g positions was found to be 0.70 volts to -0.85 volts, which roughly indicates a scale factor of 0.77 volts/g and a bias offset.

RAW AND PROCESSED DATA

The raw data collected from various sensors (GPS, IMU, data acquisition from thermisters, strain gages, ice sensors, video signals, etc.) can be stored either in the MAGI memory and/or transmitted to a ground station and/or processed onboard.

STATUS

Currently a development system has been put together using COTS components. The system consists of a four-slot backplane mounted in a cPCI chassis with a 60-watt power supply. The CPU board has a 166 MHz Pentium® processor, with 64 MB RAM, 512 KB cache; video, keyboard, mouse, serial and parallel ports, interface connectors for Ethernet, USB and FireWire. The second and third slots are occupied by two dual PCMCIA Type II slot adapter boards. Thus, there are four Type II PCMCIA slots are available. They allow the use of a flash memory card, a GPS card, a data acquisition card, and 1553 bus interface. The fourth slot of the backplane is reserved for the IMU module. Initially, the IMU module will be assembled on a wire wrap board with a built in cPCI interface.

Three iterations of the AXLGYRO processing have been completed. A device screening fixture is being fabricated so that the functionality tests could be performed on as-cut devices without the need for any bonding wires. The devices that pass the functionality tests will be packaged. A packaging trade-off study is underway using three different types of 24-pin DIP sockets. A servo trade-off analysis is underway to select and partition the servo electronics for making a universal ASIC servo chip for WADDAN SYSTEMS sensors.

CONCLUDING REMARKS

The future effort related to MAGI's development will concentrate on non-COTS modules. A chassis will be designed to meet the size constraints, and to locate the system connectors and wire harnesses. A power-conditioning module will be designed to accommodate different operational scenarios, e.g., power from the air vehicle during the flight tests, or power from an AC outlet during ground operations.

To conserve the memory resources, a small footprint operating system will be developed so that it can efficiently perform the following necessary tasks during the system boot up:

- Reorder the BUS and based upon device table reallocate resources
  - DMA
  - IRQs
  - I/O, etc.
- Memory Management
- Device Drivers/Device Drivers to be loaded on the fly
- Partition Tables
- User Process Initialization
- Access Control
- Applications Loading
- Process Scheduling

The predicted high resolution of the gyro assumes that the two orthogonal gimbal resonant frequencies will match within ±5 Hz. Initially, this is planned to be achieved by accurate photolithography during the gimbal machining step, and screening the devices by tests to meet the above frequency matching criterion. However, if this is not sufficient, a *dynamic laser-tuning step* will be introduced to actively trim the gyro structure to meet the frequency-matching requirement.

After packaging, the current version of the AXLGYROs will be mounted as a triad on an appropriate IMU board and evaluated for possible performance degradation. If this arrangement of the IMU module causes excessive noise and performance degradation due to vibration and shock, then the sensor block can be mounted off-the-board on a stiffened section of the chassis wall.

A realistic but simple bench mark test will be devised to characterize the system. A van test will be conducted to determine the effect of ground transportation on the system performance. The Kalman filter mechanization integrating the GPS/INS solutions, if necessary, will be fine-tuned using actual data collected during testing in a mobile van.

Other possible options include the development of a C-Band transponder itself or its interface as a module for MAGI. A single chip integrated inertial measurement device (IIMD) can be developed for future IMU modules.

In this paper, we presents our work in development of a unique electro-optic hybrid rotary joint for current ground-based electro-optic tracking system applications. By integrating a unique on-axis fiber optical rotary joint with a specially designed two-layer concentric electrical slip ring structure, a comprehensive EOHRJ will be produced to replace existing wrap-cable RTF structure in the current tracker systems. It is expected that, with the EOHRJ equipped, future tracker system will be able to realize rotating-to-fixed signal transmission for all types of signals channels, including electrical power,

ground, control, and feedback signals, as well as high speed video, audio, and data signals.

Besides the tracker system application, the developed EOHRJ technology will result in a generic electrical and optical slip ring architecture, on which a number of structural alternatives can be developed to numerous other military and commercial applications involving the transmission of large amounts of data and signals to and from moving platforms. Potential applications include robotics (used to fabricate automobiles and aircraft); surveillance systems (used for monitoring aircraft and automobile traffic); instrumentation and observation systems located on rotating platforms (such as turbines and jet engines); multi-spectral vision systems located on automobiles and aircraft; and flight data recorders.